

## Research Paper

# Investigation of the Effect of Viscosity and Density on the Wave Propagation of a Nonlocal Porous Beam Submerged in Fluid using Bernstein Polynomials

Thangamuni PRABHAKARAN<sup>1</sup>), Rajendran SELVAMANI<sup>1</sup>)\*,  
Madasamy MAHAVEERSREEJAYAN<sup>2</sup>), Lifeng WANG<sup>2</sup>)

<sup>1</sup>) *Department of Mathematics, Karunya Institute of Technology and Sciences*  
Coimbatore-641114, Tamil Nadu, India; e-mail: prabha251999@gmail.com

<sup>2</sup>) *State Key Laboratory of Mechanics and Control of Mechanical Structures*  
*Nanjing University of Aeronautics and Astronautics*  
210016 Nanjing, People's Republic of China;  
e-mail: mahaveersreejayan@gmail.com; walfe@nuaa.cn

\*Corresponding Author e-mail: selvam1729@gmail.com

This study investigates the effect of viscosity and density on the free vibration characteristics of a homogeneous porous Euler nanobeam submerged in fluid, incorporating the governing equations from Eringen's nonlocal elasticity theory. To enhance computational efficiency in our analysis, we employ the Rayleigh-Ritz method, utilizing computationally efficient Bernstein polynomials as shape functions. Furthermore, we explore a range of classical boundary conditions tailored to address the specific problem at hand. In order to validate our findings, we conduct a comparative analysis against existing literature, thereby underscoring the effectiveness and robustness of our proposed methodology. Our research also places a significant emphasis on elucidating the impact of nonlocal parameters, non-dimensional amplitude, thickness, density, viscosity and porosity on non-dimensional frequency across various boundary conditions, including simply-supported (S-S), clamped-simply supported (C-S), and clamped-clamped (C-C) configurations.

**Keywords:** Euler nanobeam; fluid-solid interaction; nonlocal elasticity; porous nanobeam; Bernstein polynomials; Rayleigh-Ritz method.

## 1. INTRODUCTION

The widespread adoption of nanomaterials in diverse engineering fields, such as microfabrication technology, aircraft frameworks, rocket propulsion systems, fuel cells, and microelectronics, has generated considerable interest within the scientific community. Scientists in this field focus on investigating the mechanical

properties of nanoscale structural elements such as nanobeams, nanoplates and nanoshells. Notably, the use of coupled nanobeams has progressed significantly in the realm of nanotechnology and nanodevices, leading to a comprehensive studies on the mechanical attributes of double and multiple-nanobeam systems.

In order to achieve the requisite precision in nanoresonator, PENG *et al.* [1], and nanoactuator, DUBEY *et al.* [2], introduced methods to incorporate small-scale effects and atomic forces into the systems. Research dedicated to nanobeam mechanics has revealed that conventional beam theories fall short in accurately characterizing nanobeam mechanical properties RUUD *et al.* [3]. Neglecting these small-scale effects can yield significantly flawed outcomes in nano design, resulting in substandard designs. WANG and HU [4] demonstrated that classical beam theories inadequately predict the reduction in phase velocities of wave propagation in carbon nanotubes at sufficiently high wavenumbers, where the microstructure notably influences flexural wave dispersion. To address this challenge, ERINGEN introduced nonlocal elasticity theory [5]. Subsequently, REDDY [6] reformulated various beam theories, including Euler-Bernoulli and Timoshenko beam theories, by incorporating nonlocal differential constitutive relations. The author derived equations of motion considering these nonlocal theories and provided corresponding analytical solutions for beam bending, buckling, and vibration. CHAKRAVERTY and BEHERA [7] further analyzed both static and dynamic problems of nanobeams and nanoplates.

Nonlocal elasticity theory has found extensive application in the analysis of nanostructures, including nanobeams, nanoplates, nanorings, carbon nanotubes, and more. This theory incorporates forces between atoms and internal length scales, as demonstrated by (WANG [8], WANG *et al.* [9], and ZHANG *et al.* [10]). KARMAKAR and CHAKRAVERTY [11] developed a novel nonlocal beam theory specifically designed for investigating the bending, buckling, and free vibration characteristics of nanobeams. In their study, WANG *et al.* [12] addressed the problem of free vibration in Euler-Bernoulli nanobeams using analytical methods. They conducted a comparative analysis of frequency parameters under varying scaling effect parameters and diverse boundary conditions.

PHADIKAR and PRADHAN [13] utilized finite element analysis to solve the equations governing the bending, buckling, and vibration behavior of Euler nanobeams. Their study involved computing results for nanobeams under various boundary conditions, including simply supported, clamped, and free. In the field of vibration analysis of nanostructures, various methods have been explored by different researchers. These methods include the finite element method presented in ELTAHER *et al.* [14], the application of Chebyshev polynomials within the Rayleigh-Ritz method in MOHAMMADI and GHANNADPOUR [15] and the meshless method in ROQUE *et al.* [16]. Vibration properties of functionally graded nanoplates were examined using a novel nonlocal refined four-variable

model in BELKORISSAT *et al.* [17]. Subsequently, a nonlocal zeroth-order shear deformation theory was introduced for the free vibration of functionally graded nanoscale plates resting on an elastic foundation by BOUNOUARA *et al.* [18]. In another study, PRADHAN and MURMU [19] discussed the application of nonlocal elasticity and differential quadrature method (DQM) in the flap wise bending vibration of rotating nanocantilevers.

The functional and structural significance of poroelastic materials is driving notable advancements in geological, biological, and synthetic fields. These porous materials find extensive applications in aerospace and construction models, due to their low relative density, high surface area, amplified specific strength, lightweight nature, thermal insulation properties, and good permeability. The influence of thickness stretching and porosity on the mechanical response of functionally graded beams resting on elastic foundations was thoroughly discussed by ATMANE *et al.* [20], and they introduced a computational shear displacement model for the vibration analysis of functionally graded beams with porosities in a subsequent work ATMANE *et al.* [21]. BEHERA and CHAKRAVERTY [22] delved into the free vibration of Euler and Timoshenko nanobeams using a boundary characteristic orthogonal polynomial. In a distinct study, BARATI [23] conducted research on nonlocal-strain gradient forced vibration analysis of metal foam nanoplates with uniform and graded porosities. Furthermore, in another investigation, BARATI [24] explored the vibration analysis of functionally graded nanoplates with nanovoids on a viscoelastic substrate under hygro-thermo-mechanical loading using nonlocal strain gradient theory. The impact of porosity on the free and forced vibration characteristics of graphene platelet (GPL) reinforcement composite nanostructures was investigated by POURJABARI *et al.* [25]. Free vibration analysis of microtubules as cytoskeleton components was investigated by CIVALEK and AKGOZ [26]. Discussions centred on the free and forced vibrations of shear deformable functionally graded porous beams in the work of CHEN *et al.* [27].

Currently, researchers are shedding light on the influence of fluid viscosity and density on the vibration behavior of nanobeams, placing particular emphasis on the role of nonlocal elasticity theory. SHEYKHI *et al.* [28] investigated the impact of viscosity and fluid flow on buckling behavior of nanoplates with surface energy, while considering nonlocal strain gradient elasticity theory for the free vibration analysis of embedded flexoelectric curved nanobeams. The Poisson ratio of closed-cell aluminum foams was discussed by KOVÁČIK *et al.* [29]. ARPANAHI *et al.* [30] and PARSA and MAHMOUDPOUR [31] conducted an inquiry focused on free vibration of variable thickness functionally graded material (FGM) nanobeams submerged in fluid, taking into account nonlocal surface energy effects. Size-dependent free vibration of microbeams submerged in fluid was also studied by several researchers (LI *et al.* [32], ARPANAHI *et al.* [33],

LI *et al.* [34]). The buckling behavior of nonlocal nanoplates submerged in viscous moving fluid was examined by ARPANAHI *et al.* [35]. Additionally, a review of computational modelling techniques for carbon nanotubes conveying viscous fluid was conducted by WANG and NI [36]. Finally, the nonlinear free and forced vibrations of grapheme nanoplatelet-reinforced microbeams with geometric imperfection were discussed by MIRJAVADI *et al.* [37].

As far as the authors are aware, there is a lack of research exploring the impact of viscosity and density on the wave propagation of nonlocal porous beams submerged in fluid using Bernstein polynomials. Consequently, there exists a significant scientific imperative to delve into this area and better understand the effects of viscosity and density on such wave propagation.

In this article, we analyze the vibration behavior of nonlocal porous Euler nanobeams immersed in fluid by employing the governing equations derived from Eringen's nonlocal elasticity theory. To improve computational efficiency, we utilize the Bernstein polynomials-based Rayleigh-Ritz method. To verify our results, we perform a comparative analysis with existing literature, demonstrating the effectiveness and robustness of our proposed approach. Our study also emphasizes the influence of nonlocal parameters, nondimensional amplitude, thickness, density, viscosity, and porosity on the nondimensional frequency under various boundary conditions.

## 2. MATHEMATICAL FORMULATIONS

The material properties of metals are influenced by the distribution of voids or pores. These voids can be distributed uniformly or in non-uniform patterns. In cases of non-uniform distribution, it can be further categorized as symmetric (nonuniform 1) or asymmetric (nonuniform 2). Subsequently, the forthcoming section will introduce expressions for the material properties, specifically the elastic modulus ( $E$ ) and mass density ( $\rho$ ), for metal foam [37]:

$$(2.1) \quad E = E_2 (1 - e_0 \Upsilon) \rho = \rho_2 \sqrt{(1 - e_0 \Upsilon)} \quad (\text{uniform}),$$

where

$$\Upsilon = \frac{1}{e_0} - \frac{1}{e_0} \left( \frac{2}{\pi} \sqrt{1 - e_0} - \frac{2}{\pi} + 1 \right)^2.$$

The above equation defines  $\Upsilon$  as a function of the coefficient  $e_0$ , which relates to the pore density in the metal foam. This variable  $\Upsilon$  is used in the expression for  $E$  and  $\rho$  for uniformly distributed voids in metal foam.

For non-uniform distributions, the expressions are as follows:

$$(2.2) \quad \begin{aligned} E(z) &= E_2 \left( 1 - e_0 \cos \left( \frac{\pi z}{h} \right) \right), \\ \rho(z) &= \rho_2 \left( 1 - e_m \cos \left( \frac{\pi z}{h} \right) \right) \quad (\text{nonuniform 1}), \end{aligned}$$

$$(2.3) \quad \begin{aligned} E(z) &= E_2 \left( 1 - e_0 \cos \left( \frac{\pi z}{2h} + \frac{\pi}{4} \right) \right), \\ \rho(z) &= \rho_2 \left( 1 - e_m \cos \left( \frac{\pi z}{h} + \frac{\pi}{4} \right) \right) \quad (\text{nonuniform 2}), \end{aligned}$$

where  $z$  is the spatial coordinate and  $h$  is the characteristic thickness. In the above definitions, the index 2 refers to the material property at its highest value. Also, there are two coefficients  $e_0$  and  $e_m$  related to the pore density and mass distribution:

$$(2.4) \quad e_0 = 1 - \frac{E_2}{E_1} = 1 - \frac{G_2}{G_1} e_m = 1 - \sqrt{1 - e_0}.$$

Here,  $E_1$  and  $G_1$  are the elastic modulus and shear modulus of the metal without voids, respectively. Additionally,  $E_2$  and  $G_2$  are the highest values of the elastic modulus and shear modulus in the presence of voids, respectively.

### 2.1. Bernstein polynomials (BPS)

Bernstein polynomials can be employed in numerical methods for solving differential equations or systems of equations. In this section, we state some basic properties of Bernstein polynomials. These important properties will enable us to solve the nonhomogeneous nonlinear-integro-differential Eq. (5.6). Bernstein polynomials of  $n$ th-degree on the interval  $[0, 1]$  are defined by

$$(2.5) \quad B_{i,n}(x) = \binom{n}{i} x^i (1-x)^{n-i}, \quad i = 0, 1, \dots, n, \quad x \in [0, 1],$$

where  $\binom{n}{i} = \frac{n!}{i!(n-i)!}$ . Some particular cases of Bernstein polynomials are:

$$(2.6) \quad B_{1,0}(x) = 1 - x, \quad B_{1,1}(x) = x,$$

$$(2.7) \quad B_{2,0}(x) = (1 - x)^2, \quad B_{s2,1}(x) = 2x(1 - x), \quad B_{2,2}(x) = x^2,$$

$$(2.8) \quad \begin{aligned} B_{3,0}(x) &= (1 - x)^3, & B_{3,1}(x) &= 3x(1 - x)^2, & B_{3,2}(x) &= 3x^2(1 - x), \\ B_{3,3}(x) &= x^3. \end{aligned}$$

### 2.2. Some properties of BPS

**(i) Partition of unity:** In the context of Bernstein polynomials, the partition of unity property states that for any arbitrary value of  $x$  in the interval  $[0, 1]$ , the sum of  $n + 1$  Bernstein polynomials of degree  $n$  equals one:

$$(2.9) \quad \sum_0^n B_{n,i}(x) = 1.$$

**(ii) Interval end conditions:** The interval end conditions for Bernstein polynomials typically involve specifying the values of the polynomial at the endpoints of the interval. There are different types of end conditions depending on the specific requirements of the problem being solved. Two common types of end conditions are:

$$(2.10) \quad B_{n,i}(0) = \begin{cases} 1 & \text{if } i = 0, \\ 0 & \text{if } i \neq 0, \end{cases} \quad B_{n,i}(1) = \begin{cases} 1 & \text{if } i = n, \\ 0 & \text{if } i \neq n. \end{cases}$$

**(iii) Symmetry:** Bernstein polynomials of even degree  $n$  are symmetric about the midpoint of the interval  $[0, 1]$  which is  $x = 0.5$ . Mathematically, this symmetry can be expressed as:

$$(2.11) \quad B_{n,i}(x) = B_{n,n-i}(1-x).$$

**(iv) Recurrence formula:** The recurrence formula in the context of Bernstein polynomials is a key concept used to compute Bernstein polynomials of degree  $n$  by combining two Bernstein polynomials of degree  $n - 1$ .

$$(2.12) \quad B_{n,i}(x) = (1-x)B_{n-1,i}(x) + xB_{n-1,i-1}(x).$$

**(v) Derivatives:** Using the definition of Bernstein polynomials, Eq. (2.5), the first derivative of  $n$ -th-degree BPs can be written as a linear combination of BPs with degree  $n - 1$ :

$$(2.13) \quad \frac{d}{dx} B_{n,i}(x) = n(B_{n-1,i-1}(x) - B_{n-1,i}(x)).$$

**(vi) Integration:** The integral of a Bernstein polynomial  $B_{n,i}(x)$  of degree  $n$  over the interval  $[0, 1]$  can be computed using the following formula:

$$(2.14) \quad \int_0^1 B_{n,i}(x) dx = \frac{1}{n+1}.$$

3. FORMULATION OF THE PROBLEM

The strain-displacement relation based on Euler-Bernoulli beam theory is given by:

$$(3.1) \quad \varepsilon_{xx} = -z \frac{d^2w}{dx^2},$$

where  $x$  is the longitudinal coordinate measured from the left end of the beam,  $\varepsilon_{xx}$  is the normal strain;  $z$  is the coordinate measured from the mid-plane of the beam, and  $w$  is the transverse displacement. Let  $U$  be the strain energy, which is given by [22] as:

$$(3.2) \quad U = \frac{1}{2} \int_0^L \int_A \sigma_{xx} \varepsilon_{xx} dA dx,$$

where  $\sigma_{xx}$  is the normal stress,  $A$  is the area of the cross-section of the beam, and  $L$  is the length of the beam. The bending moment is given by:

$$(3.3) \quad M = \int_A \sigma_{xx} z dA.$$

We use Eqs. (3.1) and (3.3) in Eq. (3.2), to express the maximum strain energy as:

$$(3.4) \quad U_{\max} = -\frac{1}{2} \int_0^L M \frac{d^2w}{dx^2} dx.$$

Assuming free harmonic motion, the maximum kinetic energy is obtained as:

$$(3.5) \quad T_{\max} = \frac{1}{2} \int_0^L \rho A \omega^2 w^2 dx,$$

where  $\omega$  is the circular frequency of the vibration, and  $\rho$  be the mass density of the material of the beam. The governing equation of motion, without rotary inertia, is given by [26]:

$$(3.6) \quad \frac{d^2M}{dx^2} = -\rho A \omega^2 w + F_{ext}.$$

For an elastic material in the one-dimensional case, Eringen’s nonlocal constitutive relation may be written as [11]:

$$(3.7) \quad \sigma_{xx} - (e_0a)^2 \frac{d^2\sigma_{xx}}{dx^2} = E\varepsilon_{xx},$$

where  $E$  represents Young's modulus, and  $e_0a$  denotes the nonlocal parameter that accounts for small-scale effect. The parameter  $a$  represents the internal characteristic length, for instance, the lattice parameter, C-C bond length, or granular distance. Meanwhile,  $e_0$  is a constant specific to each material. Determining the value of  $e_0$  might involve experimental measures or approximations obtained by aligning the dispersion curves of plane waves with those predicted by atomic lattice dynamics.

Now multiplying Eq. (3.7) by  $z dA$  and integrating over the area  $A$ , the following relation can be obtained:

$$(3.8) \quad M - (e_0a)^2 \frac{d^2M}{dx^2} = -EI \frac{d^2w}{dx^2},$$

where  $I$  is the second moment of inertia. Substituting Eq. (3.6) in (3.8), we get:

$$(3.9) \quad M = -EI \frac{d^2w}{dx^2} - [(e_0a)^2(\rho A \omega^2 w - F_{ext})].$$

#### 4. MODELING THE FLUID-SOLID INTERACTION

By differentiating the displacement along the  $z$ -direction, we obtain the following relations:

$$(4.1) \quad v_w = \frac{dw}{dt},$$

$$(4.2) \quad \frac{dv_w}{dt} = \frac{d^2w}{dt^2},$$

where  $v_w$  is the velocity along the  $z$ -direction. The Navier-Stokes relation [36] along the  $z$ -direction can be expressed as:

$$(4.3) \quad \rho_f \frac{dv_w}{dt} = -\nabla p + \mu_f \nabla^2 v_w,$$

where  $p$  is the fluid pressure, and  $\rho_f$  and  $\mu$  are its density and viscosity, respectively. The Navier-Stokes relation is rewritten in the following form via a delta operator expansion:

$$(4.4) \quad \rho_f \frac{dv_w}{dt} = -\frac{\partial p}{\partial z} + \mu_f \left( \frac{\partial^2 v_w}{\partial x^2} + \frac{\partial^2 v_w}{\partial y^2} + \frac{\partial^2 v_w}{\partial z^2} \right).$$

The thin beam in question obeys the Euler-Bernoulli beam assumptions [6]. As a result, Eq. (4.4) can be simplified as:

$$(4.5) \quad \rho_f \frac{dv_w}{dt} = -\frac{\partial p}{\partial z} + \mu_f \left( \frac{\partial^2 v_w}{\partial x^2} + \frac{\partial^2 v_w}{\partial y^2} \right).$$

The beam velocity in the  $z$ -direction is accordingly expressed as:

$$(4.6) \quad v_w = \frac{dw}{dt} = \frac{\partial w}{\partial t} + v_x \frac{\partial w}{\partial x} + v_y \frac{\partial w}{\partial y}.$$

Performing differentiation leads to:

$$(4.7) \quad \frac{dv_w}{dt} = \frac{\partial}{\partial t} \left( \frac{\partial w}{\partial t} + v_x \frac{\partial w}{\partial x} + v_y \frac{\partial w}{\partial y} \right) + v_x \frac{\partial}{\partial x} \left( \frac{\partial w}{\partial t} + v_x \frac{\partial w}{\partial x} + v_y \frac{\partial w}{\partial y} \right) \\ + v_y \frac{\partial}{\partial y} \left( \frac{\partial w}{\partial t} + v_x \frac{\partial w}{\partial x} + v_y \frac{\partial w}{\partial y} \right).$$

After applying the mentioned simplifications in the above equations, one obtains:

$$(4.8) \quad \frac{dw}{dt} = \frac{\partial w}{\partial t},$$

$$(4.9) \quad \frac{dv_w}{dt} = \frac{\partial^2 w}{\partial t^2}.$$

In view of  $\frac{\partial w}{\partial y} \neq 0$  and applying the delta operator to the velocity, it is found that:

$$(4.10) \quad \nabla^2 v_w = \nabla^2 \frac{dw}{dt} = \frac{\partial^3 w}{\partial x^2 \partial t}.$$

After substituting of Eqs. (4.8) and (4.10) into Eq. (4.5), the pressure gradient exerted on the beam surface from the fluid is written as:

$$(4.11) \quad \frac{\partial p}{\partial z} = -\rho_f \left( \frac{\partial^2 w}{\partial t^2} \right) + \mu_f \left( \frac{\partial^3 w}{\partial x^2 \partial t} \right).$$

To obtain the force applied to the beam from the fluid, Eq. (4.11) is multiplied by the fluid height ( $h_f$ ), and this force is taken as the external load exerted on the beam in the presented vibration model:

$$(4.12) \quad F_{ext} = q_w = (A_p) \frac{\partial p}{\partial z} = -(h_f) \rho_f \left( \frac{\partial^2 w}{\partial t^2} \right) + (h_f) \mu_f \left( \frac{\partial^3 w}{\partial x^2 \partial t} \right).$$

By substituting Eq. (4.12) in (3.9), we get:

$$(4.13) \quad M = -EI \frac{d^2 w}{dx^2} - \left[ (e_0 a)^2 \left( \rho A \omega^2 w - (h_f) \rho_f \left( \frac{\partial^2 w}{\partial t^2} \right) + (h_f) \mu_f \left( \frac{\partial^3 w}{\partial x^2 \partial t} \right) \right) \right].$$

## 5. SOLUTION METHODOLOGY

The vibration equation of the Euler nanobeam has been solved using the Rayleigh-Ritz method, with Bernstein polynomials as the basis functions. For this purpose, we introduce the following non-dimensional terms:

$$\begin{aligned} X &= \frac{x}{L}, \\ W &= \frac{w}{L} \quad (\text{non-dimensional displacement}), \\ \varsigma &= \frac{e_0 a}{L} \quad (\text{scaling effect parameter}). \end{aligned}$$

## 5.1. Bernstein-based Rayleigh-Ritz method

Here, the displacement function is assumed as:

$$(5.1) \quad W(X) = \sum_{I=0}^n c_I \varphi_I,$$

where  $c_i$  are the unknown constants and  $n$  is the order of the approximation.

The shape functions  $\varphi_i$ 's are chosen as:

$$(5.2) \quad \phi_i(X) = \eta_b B_{i,n}(X),$$

where  $B_{i,n}(X)$  are the Bernstein polynomials [7]:

$$(5.3) \quad B_{i,n}(X) = \binom{n}{i} X^i (1-X)^{n-i},$$

where  $\binom{n}{i} = \frac{n!}{i!(n-i)!}$ ; where  $i = 0, 1, \dots, n$  and  $\eta_b$  is the non-dimensional boundary polynomial for the nanobeam with different boundary conditions, which may be written as:

$$(5.4) \quad \eta_b = X^p (1-X)^q,$$

where  $p$  and  $q$  take values of 0, 1 or 2 according to whether the boundary is free, simply supported, or clamped, respectively. Thus, we can easily handle the boundary conditions of the problem by using various values of  $p$  and  $q$ . In the Rayleigh-Ritz method, we have:

$$(5.5) \quad U_{\max} = T_{\max}.$$

Substituting Eq. (5.1) into Eq. (5.5) and differentiating partially with respect to the unknown coefficients  $c_i$ , we get a generalized eigenvalue problem as:

$$(5.6) \quad \mathbf{P}\mathbf{Y} = \lambda^2\mathbf{M}\mathbf{Y},$$

where  $\lambda^2 = \frac{\rho_0 A \omega^2 L^4}{E_0 L}$  is the frequency parameter,  $\mathbf{Y} = [c_0 c_1 \dots c_n]^T$ , and the matrices  $\mathbf{M}$  and  $\mathbf{P}$  are the mass and stiffness matrices, respectively, which are given below:

$$\mathbf{P} = [p_{ij}], \quad i, j = 1, 2, \dots, n,$$

$$\mathbf{M} = [m_{ij}], \quad i, j = 1, 2, \dots, n,$$

where  $i$  is row number,  $j$  is column number and

$$p_{ij} = \int_0^1 \left( \frac{d^2\phi_i}{dx^2} \frac{d^2\phi_j}{dx^2} + \frac{\alpha^2 q w L}{EI} \frac{d^2\phi_i}{dx^2} \right) dX,$$

$$m_{ij} = \int_0^1 \left( \phi_j \phi_i - \frac{a^2}{2} \phi_j \frac{d^2\phi_i}{dx^2} - \frac{a^2}{2} \frac{d^2\phi_j}{dx^2} \phi_i \right) dX,$$

$$\phi_k = B_{k,n}(X)\eta_b(X), \quad \text{and} \quad k = i \quad \text{or} \quad k = j.$$

5.2. Solution using orthogonal Bernstein polynomials (OBPS)

We express the displacement function as:

$$(5.7) \quad W(X) = \sum_{i=0}^n c_i \widehat{\phi}_i,$$

where  $\widehat{\phi}_i$  are the orthogonal Bernstein polynomials, which are obtained via Gram-Schmidt orthogonalization as follows:

$$(5.8) \quad \theta_i = \eta_b B_{i,n}(X),$$

where  $B_{i,n}(X)$  and  $\eta_b$  are defined in Eqs. (5.3) and (5.4), respectively.

$$(5.9) \quad \widehat{\phi}_0 = \theta_0,$$

$$(5.10) \quad \widehat{\phi}_i = \theta_i - \sum_{j=0}^{i-1} \beta_{ij} \widehat{\phi}_j,$$

where

$$\beta_{ij} = \frac{\langle \theta_i, \theta_j \rangle}{\langle \widehat{\phi}_j, \widehat{\phi}_j \rangle}.$$

Here the inner product  $\langle \cdot, \cdot \rangle$  is defined as:

$$\langle \hat{\phi}_i, \hat{\phi}_j \rangle = \int_0^1 \hat{\phi}_i(X) \hat{\phi}_j(X) dX,$$

and the norm can be written as:

$$(5.11) \quad \|\hat{\phi}_i\| = \langle \hat{\phi}_i, \hat{\phi}_i \rangle^{1/2} = \left[ \int_0^1 \hat{\phi}_i(X) \hat{\phi}_i(X) dX \right]^{1/2}.$$

We now claim that the assumed displacement function in Eq. (5.1) will converge with respect to the considered shape functions, namely Bernstein polynomials (defined in Eq. (5.3)).

### 6. NUMERICAL RESULTS AND DISCUSSION

Following the determination of the closed-form vibration frequency of the porous homogeneous submerged nanobeam, depicted in Fig. 1, one can explore its dependence on several factors, including the scaling parameter, porosity pattern, and nonlocal effects. To perform this analysis, a set of material constants is provided in Tables 1 and 2.

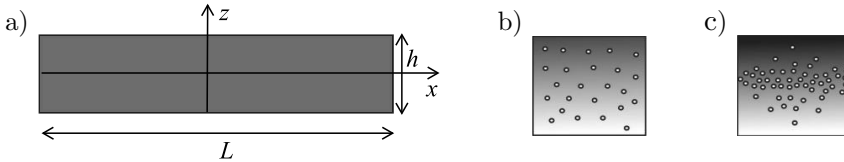


FIG. 1. (a) Geometry of the porous nanobeam, (b) uniform porosity, (c) nonuniform porosity.

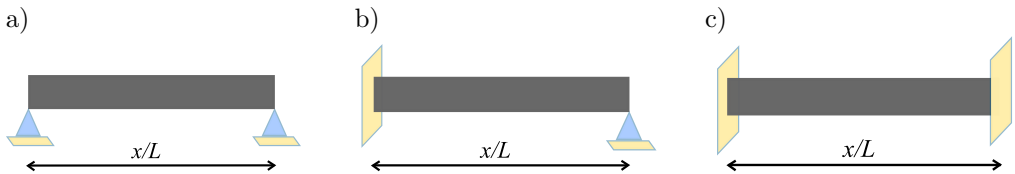


FIG. 2. Boundary conditions: a) simply-supported (S-S), b) clamped simply-supported (C-S), c) clamped-clamped (C-C).

**Table 1.** Beam dimensions and material properties [29].

$a$ [m]	$b$ [m]	$h_f$ [m]	$h$ [m]	$\rho_2$	$E_2$ [MPa]	$\nu$
0.5	0.05	0.5	0.05	2700	70	0.3

**Table 2.** Material properties of the fluid [28].

Fluid	$\mu_f$ [Pa · s]	$\rho_f$ [kg/m <sup>3</sup> ]
Water	$8.9 \times 10^{-4}$	1000
Honey	10	1420

Table 3 demonstrates the numerical results of the nondimensional frequencies across different fluid densities in various modes, computed by using boundary points (BPs) and optimal boundary points (OBPs) methods, respectively. For various fluid densities, it is observed that the frequencies decrease for higher fluid densities and become more condensed in larger modes. The BPs method achieves higher frequency values compared to the OBPs method. Furthermore, in Table 4, the first three frequency modes of submerged nanobeams are presented and these results are compared with those from [28], showing good agreement.

**Table 3.** Comparison of nondimensional frequencies using BPs and OBPs methods.

$\rho_f$	BPs			OBPs		
	Mode 1	Mode 2	Mode 3	Mode 1	Mode 2	Mode 3
(1000)	7.05318	6.83003	6.48223	6.17677	5.90547	5.66221
(1500)	3.96189	4.27347	4.04510	3.84400	3.66489	3.50383
(2000)	3.30080	3.64465	3.44566	3.27021	3.11374	2.97286
(2500)	2.86060	3.20978	3.03141	2.87397	2.73342	2.60672
(3000)	2.53468	2.87697	2.71454	2.57103	2.44278	2.32705

**Table 4.** Validation of natural frequency of submerged beam in water.

Mode number	Present study	SHEYKHI <i>et al.</i> [28]
1	294.537	295.537
2	907.354	907.464
3	1573.460	1573.460

Figures 3–5 display the dispersion of non-dimensional frequency over non-dimensional amplitudes for different porous patterns and various boundary conditions. Examining Figs. 3–5 reveals that the non-dimensional frequency undergoes significant variation with an increase in non-dimensional amplitude, with particularly enhanced values along the C-C edge. Notably, the results indicate that a nano-sized beam characterized by nonuniform pores type 2 exhibits the highest vibration frequency. In contrast, the curves for uniform nanoporous and nonuniform pores type 1 are closely aligned. These trends suggest that a nano-sized beam featuring a symmetrical void type may achieve superior beam stiff-

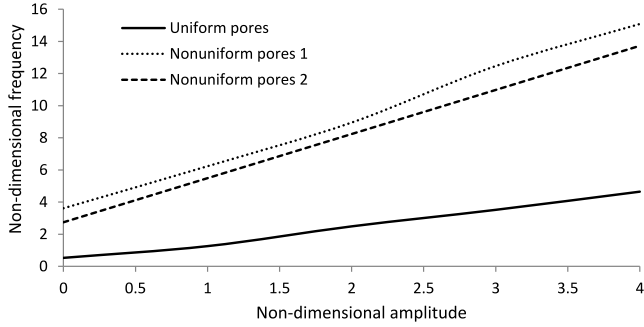


FIG. 3. Plot of non-dimensional frequency over non-dimensional amplitude for different porosity at the S-S boundary.

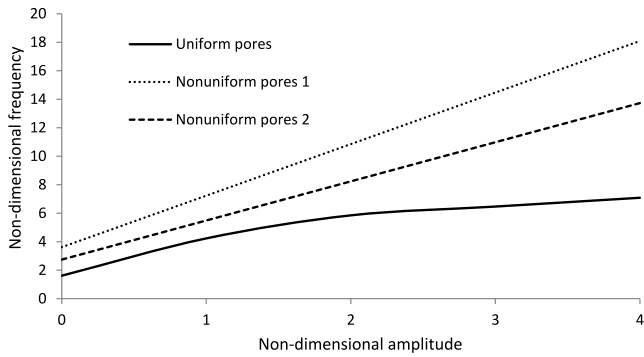


FIG. 4. Plot of non-dimensional frequency over non-dimensional amplitude for different porosity at the C-S boundary.

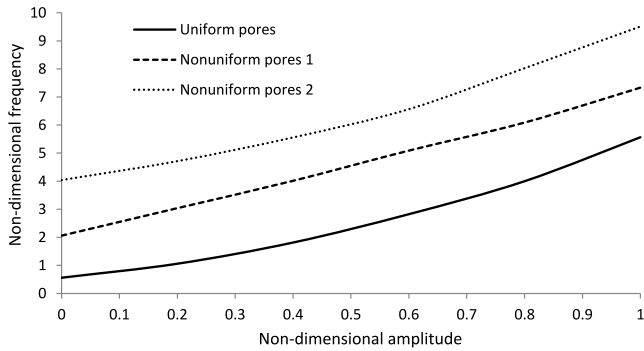


FIG. 5. Plot of non-dimensional frequency over non-dimensional amplitude for different porosity at the C-C boundary.

ness, and overall outstanding mechanical properties. This interpretation underscores the significant impact of nano-structural characteristics on the dynamic behavior and mechanical performance of the beam.

The influence of the nonlocal parameter on the non-dimensional frequency of a nonlocal beam in various fluid environments is illustrated in Figs. 6–8. The findings suggest that when the density of the fluid surrounding the beam increases, the non-dimensional frequencies decrease at a faster rate compared to those in a vacuum. Furthermore, the impact of the nonlocal parameter is more pronounced under vacuum conditions.

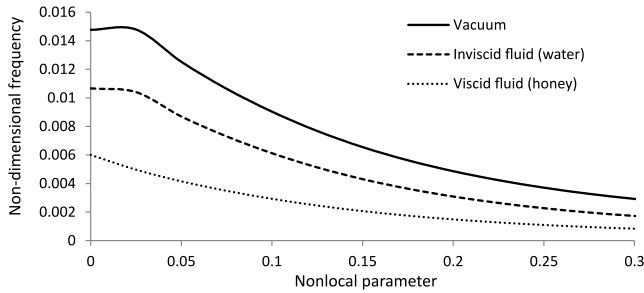


FIG. 6. Plot of non-dimensional frequency versus nonlocal parameter for different fluids at the S-S boundary.

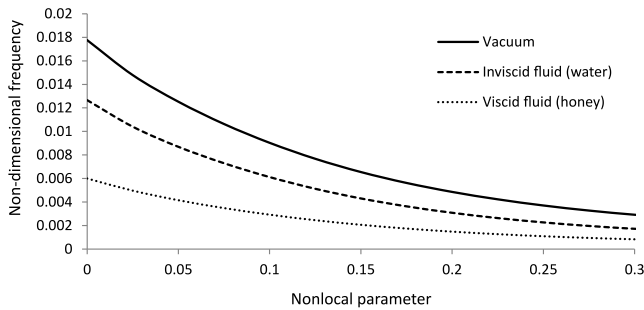


FIG. 7. Plot of non-dimensional frequency versus nonlocal parameter for different fluids at the C-S boundary.

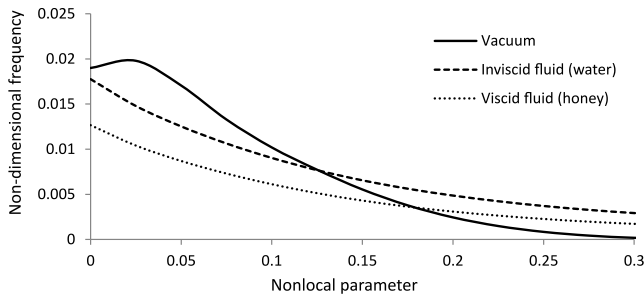


FIG. 8. Plot of non-dimensional frequency versus nonlocal parameter for different fluids at the C-C boundary.

The impact of thickness on the non-dimensional frequency of the nonlocal beam in different fluid media is shown in Figs. 9–11. The obtained results indicate that as the density of fluid in contact with the thickness increases, the non-dimensional frequencies drop more rapidly compared to those in avacuum.

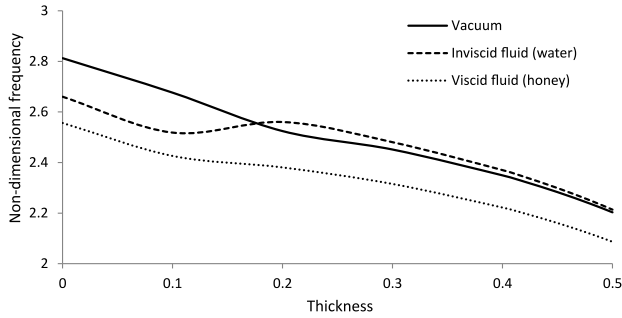


FIG. 9. Plot of non-dimensional frequencies versus thickness for different fluids at the S-S boundary.

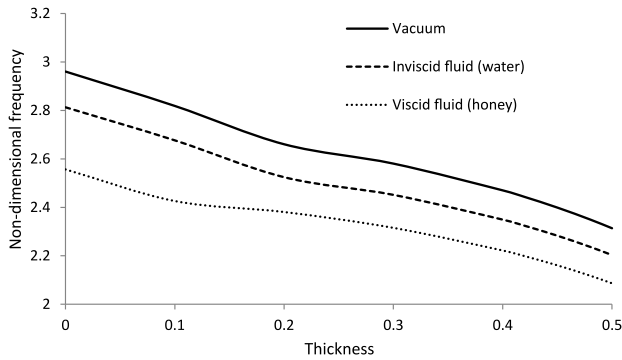


FIG. 10. Plot of non-dimensional frequencies versus thickness for different fluids at the C-S boundary.

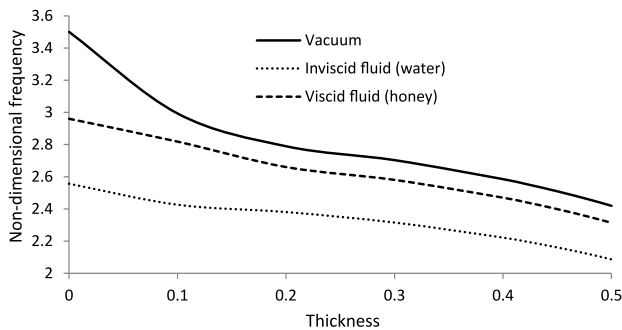


FIG. 11. Plot of non-dimensional frequencies versus thickness for different fluids at the C-C boundary.

By comparing the natural frequencies in the presence of honey, it is concluded that the ineffectiveness of fluid viscosity on the vibrational behavior of nanobeams is evident.

Figures 12–14 presents the non-dimensional frequency of the nanobeam for various fluid viscosities. As the fluid viscosity increases, the natural frequency

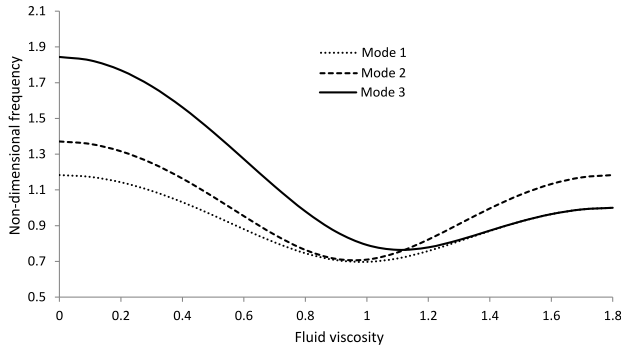


FIG. 12. Plot of non-dimensional frequency versus fluid viscosity for different modes at the S-S boundary.

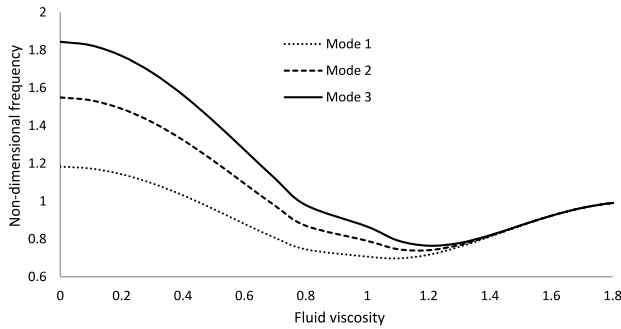


FIG. 13. Plot of non-dimensional frequency versus fluid viscosity for different modes at the C-S boundary.

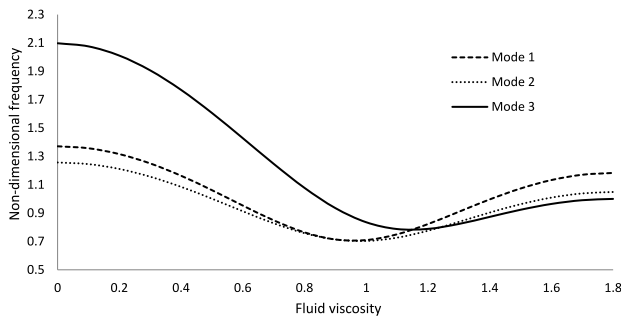


FIG. 14. Plot of non-dimensional frequency versus fluid viscosity for different modes at the C-C boundary.

decreases. The first vibration mode of the nanobeam is more affected by being submerged in fluid, followed by the second and third modes. These results suggest that, when designing dynamic aspects of nanobeams coupled with fluid, it is important to consider the viscosity of the fluid.

## 7. CONCLUSIONS

This research focused on the vibration characteristics of nonlocal porous Euler nanobeams, utilizing the governing equations from Eringen's nonlocal elasticity theory. To enhance computational efficiency, we employed the Bernstein polynomials-based Rayleigh-Ritz method. To validate our findings, we conducted a comparative analysis with existing literature, highlighting the effectiveness and robustness of our proposed methodology. Our study also placed significant emphasis on elucidating the impact of nonlocal parameters, non-dimensional amplitude, thickness, density and viscosity and porosity on non-dimensional frequency across various boundary conditions. We conclude the following:

- The non-dimensional frequency decrease with an increase in scaling effect parameters, and higher modes of vibration achieve amplified magnitudes.
- The frequency parameters are significantly affected by viscosity parameters.
- The clamped beams' non-dimensional frequency parameters increase with respect to physical variables.
- A nano-size beam with nonuniform pores type 2 resulted in a greater vibration frequency.
- The frequency parameters decrease when the nonlocal parameters increase.
- Denser fluids lead to a drop in non-dimensional frequency.

## REFERENCES

1. PENG H.B., CHANG C.W., ALONI S., YUZVINSKY T.D., ZETTL A., Ultrahigh frequency nanotube resonators, *Physical Review Letters*, **97**(8): 087203, 2006, doi: 10.1103/PhysRevLett.97.087203.
2. DUBEY A., SHARMA G., MAVROIDIS C., TOMASSONE M.S., NIKITCZUK K., YARMUSH M.L., Computational studies of viral protein nano-actuators, *Journal of Computational and Theoretical Nanoscience*, **1**(1): 18–28, 2004, doi: 10.1166/jctn.2003.003.
3. RUUD J.A., JERVIS T.R., SPAEPAN F., Nano indentation of Ag/Ni multi-layered thin films, *Journal of Applied Physics*, **75**(10): 4969–4974, 1994, doi: 10.1063/1.355787.
4. WANG L.F., HU H.Y., Flexural wave propagation in single-walled carbon nanotubes, *Physical Review B*, **71**(19): 195412, 2005, doi: 10.1103/PhysRevB.71.195412.

5. ERINGEN A.C., Nonlocal polar elastic continua, *International Journal of Engineering Science*, **10**(1): 1–16, 1972, doi: 10.1016/0020-7225(72)90070-5.
6. REDDY J.N., Nonlocal theories for bending, buckling and vibration of beams, *International Journal of Engineering Science*, **45**(2–8): 288–307, 2007, doi: 10.1016/j.ijengsci.2007.04.004.
7. CHAKRAVERTY S., BEHERA L., *Static and Dynamic Problems of Nanobeams and Nanoplates*, World Scientific, 2017.
8. WANG Q., Wave propagation in carbon nanotubes via nonlocal continuum mechanics, *Journal of Applied Physics*, **98**(12): 124301, 2005, doi: 10.1063/1.2141648.
9. WANG C.M., ZHANG Y.Y., HE X.Q., Vibration of nonlocal Timoshenko beams, *Nanotechnology*, **18**(10): 105401, 2007, doi: 10.1088/0957-4484/18/10/105401.
10. ZHANG Y.Q., LIU G.R., XIE X.Y., Free transverse vibrations of double-walled carbon nanotubes using a theory of nonlocal elasticity, *Physical Review B*, **71**(19): 195404, 2005, doi: 10.1103/PhysRevB.71.195404.
11. KARMAKAR S., CHAKRAVERTY S., Boundary characteristic Bernstein polynomials based solution for free vibration of Euler nanobeams, *Journal of Composites Science*, **3**(4): 99, 2019, doi: 10.3390/jcs3040099.
12. WANG C.M., KITIPORNCHAI S., LIM C.W., EISENBERGER M., Beam bending solution based on nonlocal Timoshenko beam theory, *Journal of Engineering Mechanics*, **134**(6): 475–481, 2008, doi: 10.1061/(ASCE)0733-9399(2008)134:6(475).
13. PHADIKAR J.K., PRADHAN S.C., Variational formulation and finite element analysis for nonlocal elastic nanobeams and nanoplates, *Computational Materials Science*, **49**(3): 492–499, 2010, doi: 10.1016/j.commatsci.2010.05.040.
14. ELTAHER M.A., EMAM S.A., MAHMOUD F.F., Free vibration analysis of functionally graded size-dependent nanobeams, *Applied Mathematics and Computation*, **218**(14): 7406–7420, 2012, doi: 10.1016/j.amc.2011.12.090.
15. MOHAMMADI B., GHANNADPOUR S.A.M., Energy approach vibration analysis of nonlocal Timoshenko beam theory, *Procedia Engineering*, **10**: 1766–1771, 2011, doi: 10.1016/j.proeng.2011.04.294.
16. ROQUE C.M.C., FERREIRA A.J.M., REDDY J.N., Analysis of Timoshenko nanobeams with a nonlocal formulation and meshless method, *International Journal of Engineering Science*, **49**(9): 976–984, 2011, doi: 10.1016/j.ijengsci.2011.05.010.
17. BELKORISSAT I., HOUARI M.S.A., TOUNSI A., ADDA BEDIA E.A., MAHMOUD S.R., On vibration properties of functionally graded nano-plate using a new nonlocal refined four variable model, *Steel Composite Structures*, **18**(4): 1063–1081, 2015, doi: 10.12989/scs.2015.18.4.1063.
18. BOUNOUARA F., BENRAHOU K.H., BELKORISSAT I., TOUNSI A., A nonlocal zeroth-order shear deformation theory for free vibration of functionally graded nanoscale plates resting on elastic foundation, *Steel and Composite Structures*, **20**(2): 227–249, 2016, doi: 10.12989/scs.2016.20.2.227.
19. PRADHAN S.C., MURMU T., Application of nonlocal elasticity and DQM in the flapwise bending vibration of a rotating nanocantilever, *Physica E: Low-dimensional systems and Nanostructures*, **42**(7): 1944–1949, 2010, doi: 10.1016/j.physe.2010.03.004.

20. ATMANE H.A., TOUNSI A., BERNARD F., Effect of thickness stretching and porosity on mechanical response of a functionally graded beams resting on elastic foundations, *International Journal of Mechanical and Materials in Design*, **13**(1): 71–84, 2017, doi: 10.1007/s10999-015-9318-x.
21. ATMANE H.A., TOUNSI A., BERNARD F., MAHMOUD S.R., A computational shear displacement model for vibrational analysis of functionally graded beams with porosities, *Steel and Composite Structures*, **19**(2): 369–384, 2015, doi: 10.12989/scs.2015.19.2.369.
22. BEHERA L., CHAKRAVERTY S., Free vibration of Euler and Timoshenko nanobeams using boundary characteristic orthogonal polynomial, *Applied Nanoscience*, **4**(3): 347–358, 2014, doi: 10.1007/s13204-013-0202-4.
23. BARATI M.R., Nonlocal-strain gradient forced vibration analysis of metal foam nanoplates with uniform and graded porosities, *Advances in Nano Research*, **5**(4): 393–414, 2017, doi: 10.12989/anr.2017.5.4.393.
24. BARATI M.R., Vibration analysis of FG nanoplates with nanovoids on viscoelastic substrate under hygro-thermo-mechanical loading using nonlocal strain gradient theory, *Structural Engineering and Mechanics*, **64**(6): 683–693, 2017, doi: 10.12989/sem.2017.64.6.683.
25. POURJABARI A., HAJILAK Z.E., MOHAMMADI A., HABIBI M., SAFARPOUR H., Effect of porosity on free and forced vibration characteristics of the GPL reinforcement composite nanostructures, *Computers & Mathematics with Applications*, **77**(10): 2608–2626, 2019, doi: 10.1016/j.camwa.2018.12.041.
26. CIVALEK O., AKGOZ B., Free vibration analysis of microtubules as cytoskeleton components: nonlocal Euler-Bernoulli beam modeling, *Iranian Journal of Science and Technology, Transaction B: Mechanical Engineering*, **17**: 367–375, 2010.
27. CHEN D., YANG J., KITIPORNCHAI S., Free and forced vibrations of shear deformable functionally graded porous beams, *International Journal of Mechanical Sciences*, **108–109**: 14–22, 2016, doi: 10.1016/j.ijmecs.2016.01.025.
28. SHEYKHI M., ESKANDARI A., GHAFARI D., ARPANAHI R.A., MOHAMMADI B., HASHEMI S.H., Investigation of fluid viscosity and density on vibration of nano beam submerged in fluid considering nonlocal elasticity theory, *Alexandria Engineering Journal*, **65**: 607–614, 2023, doi: 10.1016/j.aej.2022.10.016.
29. KOVÁČIK J., MARSAVINA L., LINUL E., Poisson’s ratio of closed-cell aluminium foams, *Materials*, **11**(10): 1904, 2018, doi: 10.3390/ma11101904.
30. ARPANAHI R.A., HOSSEINI-HASHEMI S., RAHMANIAN S., HASHEMI S.H., AHMADI-SAVADKOOHI A., Nonlocal surface energy effect on free vibration behavior of nanoplates submerged in incompressible fluid, *Thin-Walled Structures*, **143**: 106212, 2019, doi: 10.1016/j.tws.2019.106212.
31. PARSA A., MAHMOUDPOUR E., Nonlinear free vibration analysis of embedded flexoelectric curved nanobeams conveying fluid and submerged in fluid via nonlocal strain gradient elasticity theory, *Microsystem Technologies*, **25**: 4323–4339, 2019, doi: 10.1007/s00542-019-04408-0.
32. LI H.C., KE L.L., YANG J., KITIPORNCHAI S., WANG Y.S., Free vibration of variable thickness FGM beam submerged in fluid, *Composite Structures*, **233**: 111582, 2020, doi: 10.1016/j.compstruct.2019.111582.

33. ARPANAHI R.A., ESKANDARI A., MOHAMMADI B., HASHEMI S.H., Study on the effect of viscosity and fluid flow on buckling behavior of nanoplate with surface energy, *Results in Engineering*, **18**: 101078, 2023, doi: 10.1016/j.rineng.2023.101078.
34. LI H.C., KE L., YANG J., KITIPORNCHAI S., Size-dependent free vibration of microbeams submerged in fluid, *International Journal of Structural Stability and Dynamics*, **20**(12): 2050131, 2020, doi: 10.1142/S021945542050131X.
35. ARPANAHI R.A., MOHAMMADI B., AHMADIAN M.T., HASHEMI S.H., Study on the buckling behavior of nonlocal nanoplate submerged in viscous moving fluid, *International Journal of Dynamics and Control*, **11**(6): 2820–2830, 2023, doi: 10.1007/s40435-023-01166-w.
36. WANG L., NI Q., A reappraisal of the computational modelling of carbon nanotubes conveying viscous fluid, *Mechanics Research Communications*, **36**(7): 833–837, 2009, doi: 10.1016/j.mechrescom.2009.05.003.
37. MIRJAVADI S.S., AFSHARI B.M., BARATI M.R., HAMOUDA A.M.S., Nonlinear free and forced vibrations of graphene nanoplatelet reinforced microbeams with geometrical imperfection, *Microsystem Technologies*, **25**: 3137–3150, 2019, doi: 10.1007/s00542-018-4277-4.

*Received March 22, 2024; accepted version August 15, 2024.*

*Online first September 26, 2024.*



Copyright © 2024 The Author(s).  
Published by IPPT PAN. This work is licensed under the Creative Commons Attribution License  
CC BY 4.0 (<https://creativecommons.org/licenses/by/4.0/>).